
Robust Single-Agent Reinforcement Learning for Regional Traffic Signal Control Under Demand Fluctuations

Qiang Li¹, Jin Niu² and Lina Yu*

¹ College of Urban Transportation and Logistics, Shenzhen Technology University, Shenzhen, Guangdong 518118, China

* Corresponding Authors, email: yulina@sztu.edu.cn

ABSTRACT

Traffic congestion, primarily driven by intersection queuing, significantly impacts urban living standards, safety, environmental quality, and economic efficiency. While Traffic Signal Control (TSC) systems hold potential for congestion mitigation, traditional optimization models often fail to capture real-world traffic complexity and dynamics. This study introduces a novel single-agent reinforcement learning (RL) framework for regional adaptive TSC, circumventing the coordination complexities inherent in multi-agent systems through a centralized decision-making paradigm. The model employs an adjacency matrix to unify the encoding of road network topology, real-time queue states derived from probe vehicle data, and current signal timing parameters. Leveraging the efficient learning capabilities of the DreamerV3 world model, the agent learns control policies where actions sequentially select intersections and adjust their signal phase splits to regulate traffic inflow/outflow, analogous to a feedback control system. Reward design prioritizes queue dissipation, directly linking congestion metrics (queue length) to control actions. Simulation experiments conducted in SUMO demonstrate the model's effectiveness: under inference scenarios with multi-level (10%, 20%, 30%) Origin-Destination (OD) demand fluctuations, the framework exhibits robust anti-fluctuation capability and significantly reduces queue lengths. This work establishes a new paradigm for intelligent traffic control compatible with probe vehicle technology. Future research will focus on enhancing practical applicability by incorporating stochastic OD demand fluctuations during training and exploring regional optimization mechanisms for contingency events.

Keywords: Traffic signal control (TSC), Reinforcement learning (RL), Single-agent, Queue length, Demand fluctuation resistance,

1.INTRODUCTION

Traffic congestion significantly undermines urban living quality, traffic safety, environmental conditions, and economic vitality, becoming a critical challenge for cities worldwide. A primary driver of urban road congestion is intersection queuing. Traffic Signal Control (TSC) systems are pivotal in regulating traffic flow at signalized intersections, holding great potential to ease congestion and boost travel efficiency.

Historically, traffic engineers have sought to optimize signal timings by building optimization models based on specific traffic dynamics assumptions (1). While these models simplify TSC problems, they often deviate from real-world scenarios. This disconnect prevents them from capturing the complexity and stochasticity of urban traffic, limiting their capacity to adapt swiftly to dynamic demand changes (2).

Traffic congestion significantly affects urban living standards, traffic safety, environmental quality, and economic efficiency, posing a critical challenge for cities worldwide. A major source of urban road congestion is intersection queuing. Traffic Signal Control (TSC) systems are vital for regulating traffic at signalized intersections, with great potential to reduce congestion and enhance travel efficiency.

Traditionally, traffic engineers optimized signal timings via models built on specific traffic dynamics assumptions (1). While these models simplify TSC problems, they often deviate from real-world conditions, failing to capture urban traffic's complexity and stochasticity and limiting rapid adaptation to dynamic demands (2).

Advances in artificial intelligence have spurred reinforcement learning (RL), a promising data-driven approach, to address limitations of traditional model-based control (3). Extensive research has established RL as a key technology for smart TSC systems (4-5), demonstrating strong suitability for managing complex, dynamic traffic environments (1, 6-8).

In the context of controlling multiple intersections, researchers generally recognize that as the state and action spaces expand rapidly in scale, achieving effective control via a single-agent framework becomes exceedingly challenging. For this reason, attention has shifted toward multi-agent control systems, which have shown considerable scalability potential (7, 9, 10)

Yet, deploying multi-agent systems represents merely a suboptimal approach to addressing scalability. Traffic Signal Control (TSC) is inherently governed by a single central control center (agent), which is capable of monitoring traffic conditions across all roads in the study area and coordinating the control of all intersections. This stands in fundamental contrast to the coordination of drones or Automated Guided Vehicles (AGVs).

Probe vehicle technology is currently a highly feasible traffic monitoring solution for TSC systems (11). First, its data covers most urban roads, eliminating the need for additional equipment to collect traffic information. Leveraging ride-hailing vehicles and navigation system users enables real-time trajectory collection for 10%–30% of network vehicles. Second, it can assess queue length—a key metric reflecting urban road congestion that is hard to capture with existing sensors like induction loops (12). Thus, integrating TSC methods with probe vehicle systems will expedite their large-scale application.

This study presents a regional traffic signal control (TSC) model based on single-agent reinforcement learning (RL), compatible with probe vehicle technology, differing from the dominant multi-agent frameworks in prior research. Key contributions are:

- We propose a single-agent RL model for regional TSC, where a single agent manages signal timing across multiple intersections—distinct from conventional multi-agent RL. It achieves simplicity by eliminating inter-agent coordination overhead and maintaining a unified policy optimization process.
- In the RL environment design, state and reward functions are based on queue length, with actions directly regulating it to accelerate policy learning. The queue length definition here, slightly different from traditional ones, is closely linked to congestion states and enables reliable estimation using probe vehicle link travel time data, endowing the method with potential for deployment on most urban roads.
- A simulation experiment validated the model using synthetic datasets. With fixed OD demand during training, 10%, 20%, and 30% multi-level OD demand fluctuations were introduced in inference. Results show the DreamerV3 framework effectively supports model training, exhibiting anti-fluctuation capability and reliable support for TSC learning/optimization, while effectively reducing queue length in urban road network TSC.

The remainder of this paper is structured as follows. Section 2 summarizes the related works. Section 3 delineates the RL-based TSC model. Section 4 describes the experiment design. Section 5 presents the experimental results and discussion. Finally, Section 6 concludes this work.

2.RELATED WORKS

Optimal control approaches for Traffic Signal Control (TSC) aim to determine effective signal timings to enhance traffic flow, necessitating adaptive timing to alleviate congestion and waiting times. However, their effectiveness is challenged by complex intersections, variable traffic volumes, and competing optimization objectives (9).

Traditionally, traffic engineers addressed signal optimization by formulating models predicated on specific traffic flow assumptions (13-16). These simplifications often neglect real-world uncertainties, resulting in methods poorly suited to dynamic demand patterns (2).

Recent advances in Reinforcement Learning (RL) have demonstrated strong capabilities in varied domains like robotics, autonomous systems, and game AI. This success has spurred growing application of deep RL frameworks to the demanding TSC problem, yielding encouraging outcomes (7, 9, 17).

However, scaling TSC to large networks presents significant difficulties. As the number of intersections grows, the state-action space dimensionality increases dramatically, hindering the identification of critical information and the discovery of optimal control policies (9).

Current research predominantly employs multi-agent RL (MARL) strategies, categorized as independent or collaborative. Independent MARL agents train in isolation, while collaborative MARL incorporates coordination mechanisms such as message exchange.

Chu et al. (18) proposed IA2C using separate A2C agents, subsequently stabilizing it into MA2C by integrating Adjacent Intersection Fingerprint and a Spatial Discount Factor—capturing neighbor policies/traffic states while emphasizing local rewards.

Chen et al. (10) introduced a decentralized RL framework for city-scale TSC, validated in Manhattan, New York, encompassing 2,510 signals—the largest experiment reported. Agents optimize vehicle distribution and maximize system throughput by minimizing the "pressure" metric (19-20).

Independent MARL offers key advantages in scalability. Yet, a core limitation stems from each agent's reliance solely on its local, dynamically changing environment—perturbed by other agents' actions and learning—resulting in training instability (non-stationarity) (9).

Collaborative MARL, in contrast, employs coordinated agents to manage multiple intersections, learning system-wide optimal policies. Effective coordination necessitates communication, requiring agents to share information. Bokade et al. (21) introduced the QRC-TSC framework, enabling agents to learn selective communication policies that exchange variable-length messages with minimized overhead.

To improve coordination and mitigate congestion, Yan et al. (22) proposed the Graph Cooperation Q-learning Network (GCQN-TSC) model. This approach integrates self-attention mechanisms, allowing agents to dynamically focus based on real-time traffic, thereby enhancing environmental awareness and coordination efficiency.

While previous methods often segmented traffic networks into static regions for global coordination, such fixed partitions cannot adapt to changing traffic. Addressing this limitation, Ma and Wu (23) presented a new MARL approach with adaptive network partitioning..

Notably, most existing agent-based traffic signal optimization studies have overlooked how demand fluctuations affect algorithms (24, 25). Traffic demand varies significantly with time, weather, and special events—for instance, surging during rush hours and dropping sharply in off-peak periods (24).

Current algorithms often assume stable demand, a simplification that eases design but fails in real scenarios. When demand fluctuates, these algorithms struggle to adapt, resulting in inefficient signal timing: they may cause congestion during peak surges or unnecessary waits in low-demand periods (24). This gap limits their practicality in dynamic traffic environments.

Traffic Signal Control (TSC) is inherently a single-agent problem, adequately addressed by centralized control. Multi-agent approaches may misrepresent the underlying problem, introducing unnecessary complexity through partial observability and communication overhead. Modern single-agent RL techniques can now effectively handle TSC's extensive state-action spaces, representing a more natural fit for the problem's structure. Furthermore, to enhance applicability in real-world settings, future research should analyze how Origin-Destination (OD) demand fluctuations impact the algorithm's robustness, evaluating the stability of this centralized approach.

3.METHODOLOGY

We employ a single-agent Reinforcement Learning (RL) approach to tackle regional Traffic Signal Control (TSC). RL involves an agent interacting with an environment to learn

optimal control policies through exploratory interactions, obviating the need for prior knowledge of the environment's dynamics.

All key notations are defined in Table 1.

During each training iteration at time step t , the agent observes the current environment state S_t . This state encodes essential traffic dynamics required for optimal decision-making. Based on S_t , the agent selects and executes an action a_t . Consequently, the environment transitions to a new state S_{t+1} , and the agent receives both this new state and a scalar reward r_{t+1} . This reward quantifies the action's efficacy within the environment. Utilizing this iterative interaction framework and a policy optimization algorithm, the agent progressively optimizes its action-selection policy to achieve the defined control objectives.

The iterative process of applying RL to TSC is illustrated in Figure 1.

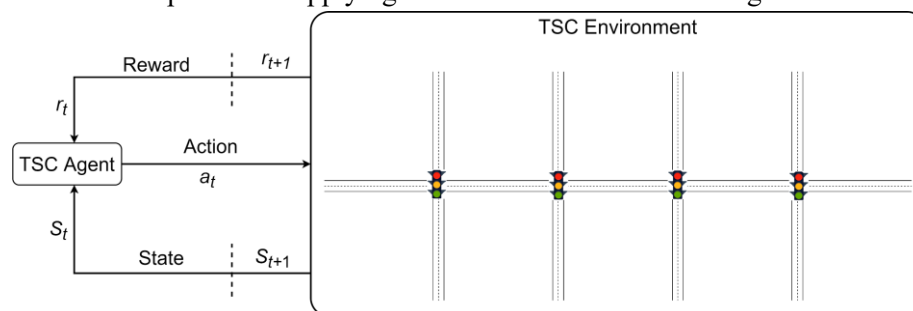


Figure 1. Single-agent RL architecture for regional traffic signal control.

This framework underscores that RL-based TSC necessitates defining five core components: state representation, action design, reward formulation, environment model, and the policy learning algorithm.

Table 1. Table of notations

Notations	Explanation
a	The action of the agent
S	The state observed by the agent
r	The reward obtained by the agent
q	The queue length of a link
t	The total travel time of all vehicles in the region
q_{ub}	The upper bound of queue length
L	The number of links in the region
s_{lb} and s_{ub}	The lower and upper bounds of the signal phase split
Δs	The phase split adjustment magnitude
M	The number of signal intersections in the region
q_{lc} and q_{hc}	The thresholds for light and heavy congestion, respectively
w_l	The link importance weight
w_{cp}	The penalty weight associated with heavy congestion
w_t	The travel time penalty weight

3.1 State

The state comprises two components: the congestion state and the signal phase scheme which are combined and represented as a single matrix.

Congestion state of a link:

The congestion state of a road link is measured by its current queue length q . This metric is physically linked to the specific roadway segment and directly reflects the monitored infrastructure. Queue length is bounded between 0 and a predefined upper limit q_{ub} .

Figure 2 depicts the spatio-temporal trajectories of a vehicle platoon entering a link and proceeding straight through consecutive intersections within a single green phase (termed the "through platoon"), alongside queued vehicles at the downstream intersection. This work defines queue length as the count of queued vehicles. Crucially, q exhibits a strong correlation with the through platoon's average travel time: Queued vehicles require green time to discharge, meaning longer queues cause more through platoon vehicles to encounter the subsequent red phase, increasing travel delay. Therefore, queue length serves as an effective link congestion metric.

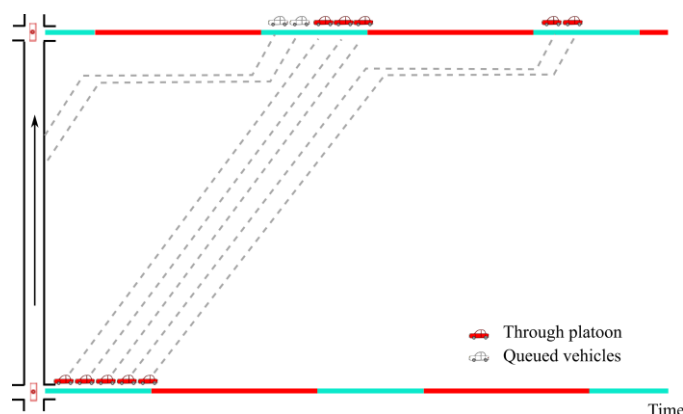


Figure 2. The definition of queue length

The queue length metric is primarily adopted due to its feasibility of estimation with minimal probe vehicle data. Prior studies have developed methods to estimate average link travel time (26) and queue length (12) using floating car data. Space constraints preclude detailing these methods here. Crucially, within these estimation frameworks, probe vehicles (floating cars) represent a sample of the through platoon. The sole inputs are the link travel times reported by these probe vehicles, utilizing only aggregated travel time data (excluding raw trajectory points).

Signal phase scheme:

The current signal phase scheme is defined as the signal phase split for each regional intersection, specifying the time allocation for traffic movements at this specific junction. The signal phase split is constrained between α and β , established beforehand.

In this study, each intersection is controlled by a four-phase signal (see Figure 3). It is assumed that the signal cycle, left-turn phase duration, yellow time, all-red time, and offset time are predetermined and fixed. The signal phase split is the only adjustable variable and defined as the sum of the north-south phases' time, which includes the north-south straight/right turn phase (Phase 1) and the left-turn phase (Phase 2). Given the signal cycle is constant, adjusting

the signal phase split regulates traffic flow at upstream and downstream intersections, managing congestion levels. As shown in Figure 3, if congestion occurs on the link indicated by the arrow (from intersection m to $m + 1$), the congestion can be alleviated by reducing the number of vehicles entering this link by increasing the signal phase split at the upstream intersection (m), or by increasing the number of vehicles exiting this link by decreasing the signal phase split at the downstream intersection ($m + 1$).

The current signal phase scheme defines the phase split for each regional intersection, specifying time allocation for traffic movements at that junction. The phase split is bounded between predefined limits s_{lb} and s_{ub} .

This study employs a four-phase signal control at each intersection (Figure 3). Signal cycle length, left-turn phase duration, yellow time, all-red time, and offset are assumed fixed and predetermined. The adjustable phase split is defined as the combined duration of the north-south phases: straight/right-turn (Phase 1) and left-turn (Phase 2). Given a fixed cycle length, adjusting this split regulates upstream and downstream traffic flow to manage congestion. For instance, congestion on the link from intersection m to $m+1$ (arrow, Figure 3) can be mitigated by either:

- Reducing inflow: Increasing the phase split at upstream intersection m reduces vehicles entering the congested link.
- Increasing outflow: Decreasing the phase split at downstream intersection $m+1$ increases vehicles exiting the link.

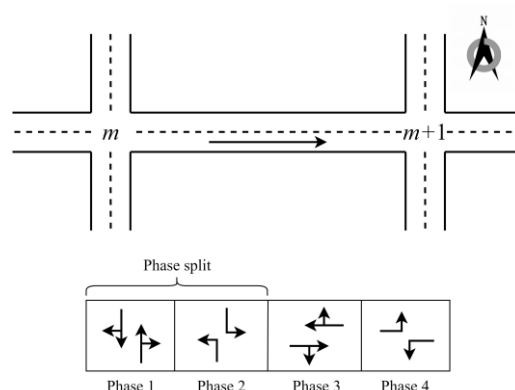


Figure 3. The signal phase split

Regional state representation:

The observed system state is represented as an $M \times M$ adjacency matrix. Diagonal elements store signal timing parameters for each intersection, while off-diagonal entries capture real-time traffic metric q for physically connected road segments; all other positions are zero. For example, in a 3×3 intersection grid (9 nodes), the 9×9 matrix has signal parameters on the diagonal, with element (1,2) denoting queue length q for the link between intersections 1 and 2.

Analogous to graph adjacency matrices, this structure explicitly preserves the transportation network's topological connectivity through spatial element distribution. Non-

zero q entries (e.g., row 1, column 2) correspond to physical inter-intersection links, while zero entries (e.g., row 1, column 7) directly indicate no connection. The spatial arrangement of q values and zeros inherently retains the network's connectivity graph, mapping intersections to nodes and non-zero q positions to edges.

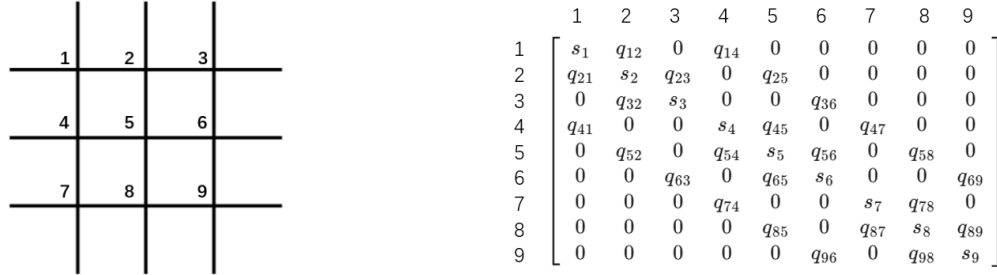


Figure 4. 3×3 Intersection State Visualization Diagram and 3×3 Intersection Grid Layout Diagram

The adjacency matrix is selected for its intrinsic capacity to unify signal parameters and traffic states q within a single representation. This structure inherently encodes network connectivity through the spatial pattern of its non-zero and zero entries. Illustrated by the 3×3 grid example, the arrangement of diagonal signal parameters and off-diagonal q values/zeros explicitly captures both individual intersection states and overall network topology.

3.2 Action

Action execution occurs sequentially: first selecting an intersection, then adjusting its phase split.

For the selected intersection, the agent can increment the current signal phase split by $-\Delta s$, 0, or $+\Delta s$, where Δs is a predefined step size. These adjustments accumulate, enabling the phase split to reach its predefined bounds s_{lb} and s_{ub} .

With M intersections, the action space size is $M \times 3$. This linear scaling with M avoids the prohibitive growth associated with simultaneous adjustments across all intersections, which would yield an action space of 3^M .

3.3 Reward

The reward function utilizes queue length q as the congestion indicator for each link. To achieve the dual objectives of congestion mitigation and total travel time minimization, the design incorporates a penalty weight under heavy congestion.

The regional reward aggregates the individual link rewards within the region. Each link's reward is computed as (Eq. 1):

$$\begin{cases} q \leq q_{lc} \text{ (Free flow): } reward = 0 \\ q_{lc} \leq q \leq q_{hc} \text{ (Light congestion): } reward = -(w_l \times q) \\ q \geq q_{hc} \text{ (Heavy congestion): } reward = -(w_{cp} \times w_l \times q) \end{cases} \quad (1)$$

Where q is the queue length of a link, q_{lc} and q_{hc} are the thresholds for light and heavy congestion, respectively. w_l represents the link importance weight and w_{cp} is the

penalty weight associated with heavy congestion. The values of q_{lc} , q_{hc} , w_l and w_{cp} are predetermined constants.

3.4 Environment

The TSC environment was developed using Gymnasium (27), an open-source Python library designed for RL algorithm development and benchmarking. Its standardized API facilitates seamless interaction between learning agents and the environment.

The observation space utilizes the previously defined adjacency matrix-like structure, with each element normalized to the range $[0, 1]$ based on its specific bounds. The action space is discretized, resulting in a total of $3 \times M$ integer actions.

The core components of the TSC environment are a traffic simulation model, a simulation controller, and a traffic monitor. The traffic simulation model must accurately replicate the target region's physical characteristics, including road geometries, intersection layouts, and traffic demand patterns, to enable effective signal timing optimization. The simulation controller handles essential operations such as executing the simulation model and deploying signal control schemes. The traffic monitor is responsible for collecting queue length data for all road segments within the region.

During the RL strategy learning phase, queue lengths are estimated directly from vehicle trajectory data generated by the simulation itself, bypassing the need for probe vehicle technology; this approach is feasible and practical for training. For consistency during model evaluation, this same simulation-based estimation method is employed. Given the established reliability of probe-based queue length estimation techniques in practice, this methodological simplification is expected to have a negligible impact on the evaluation outcomes.

At a specific control time t , the queue length on a given road segment comprises vehicles categorized into two groups based on specific criteria (Figure 5). The first group consists of vehicles that will pass through the segment: these vehicles must be proceeding straight through the downstream intersection, have entered the segment before the start time of the most recent green phase at the upstream intersection (t_{gs}^u), and have departed the segment after the start time of the next green phase at the downstream intersection (t_{gs}^d). The second group consists of vehicles remaining on the segment: these vehicles must intend to proceed straight through the downstream intersection and have entered the segment before (t_{gs}^u).

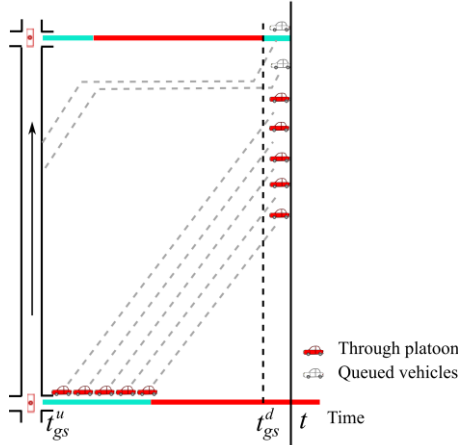


Figure 5. The queued vehicles on a road segment

3.5 DreamerV3

After testing algorithms like PPO, DreamerV3 was chosen for optimal policy training. Traditional reinforcement learning algorithms require extensive environmental interaction to develop optimized strategies, posing challenges for large-scale applications due to excessive data and computational demands.

Recent modern world models, as demonstrated by Hafner et al. (28-30), show exceptional potential for data-efficient learning in simulations and games. DreamerV3, the latest iteration, offers attractive features for policy learning (28): it synthesizes comprehensive environmental dynamics, enabling future consequence prediction through imagination to reduce real-world interaction, saving resources and accelerating learning; it only requires tuning two hyperparameters (training ratio and model size) – higher ratios improve data efficiency, while larger models enhance both final performance and efficiency – simplifying tuning for researchers.

DreamerV3 comprises World Model Learning and Actor Critic Learning (28,30,31).

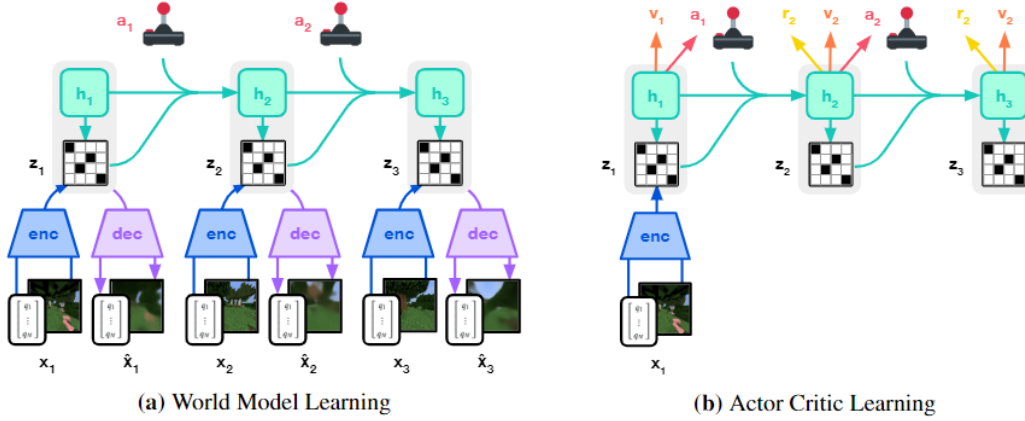


Figure 6. The DreamerV3 algorithm(27)

DreamerV3 employs a Recurrent State-Space Model (RSSM) for environment representation. It encodes observation x_t into z_t . The recurrent state h_t (updated via a_{t-1}) predicts. The combined state $s_t \doteq \{h_t, z_t\}$ predicts reward r_t , continuation $c_t \in \{0,1\}$, and reconstructs observations.

The actor and critic networks utilize world model-imagined trajectories. Both operate on s_t , leveraging the RSSM's learned representations.

4. EXPERIMENT DESIGN

4.1 Simulation setup

Experiments employ SUMO, a versatile traffic simulator, using its Python API (libsumo). This interface enables the simulation controller to execute simulations, access real-time data, and deploy signal schemes. Mesoscopic simulation mode is used, modeling queue-influenced vehicle movements at $100\times$ microscopic speed.

The RL-based TSC method is evaluated in the region shown in Figure 7. Links feature three lanes, widening to four lanes approaching downstream intersections. Each approach has:

two straight lanes, one dedicated left-turn lane, and one dedicated right-turn lane. Intersections use fixed-sequence four-phase control with: 100s cycle, 8s left-turn phase, 2s yellow, and 2s all-red. Initial phase split is 50s.

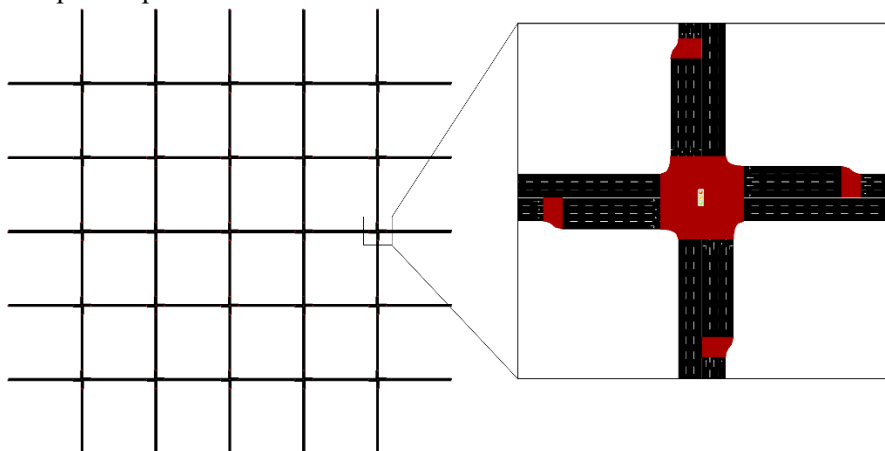


Figure 7. Region Diagram

Traffic demand is generated via zone-to-zone flows using Traffic Assignment Zones (TAZs) and an origin-destination (OD) matrix.

Figure 3 depicts the study region's geometry. Links feature three lanes, widening to four lanes approaching downstream intersections — a configuration typical of urban infrastructure to handle intersection traffic volumes. Each approach provides: two straight lanes, one left-turn lane, and one right-turn lane.

All intersections employ fixed-sequence four-phase control. Fixed timing parameters are: 100s cycle, 8s left-turn phase, 2s yellow, and 2s all-red. The initial signal phase split is set to 50 seconds, which serves as a starting point for evaluating the effectiveness of the proposed traffic signal control model.

4.2 RL-model parameter setting

Table 2 lists the parameters of the RL-based TSC model. When the signal phase split is set to its initial value (50 seconds), the saturated flow per cycle for the straight lanes is 50 vehicles. The upper bound of the queue length is set to this level. This situation is considered extreme congestion because queued vehicles consume the entire green time, forcing all incoming vehicles to stop at the downstream intersection. The thresholds for light and heavy congestion (q_{lc} and q_{hc}) are set to 20% and 50% of this saturated flow level. In scenario 1, where the major traffic flows west to east, link-importance weights (w_l) are set to 0 for links in the opposing direction. This confines the reward calculation to links aligned with the main flow.

Table 2. RL-based TSC method parameters

Parameter	Value
q_{ub}	50 no. of vehicles
q_{lc} and q_{hc}	10 and 25 no. of vehicles (20 % and 50 % of q_{ub} , respectively)
s_{lb} and s_{ub}	30 s and 70 s
Δs	2 s

w_l	0 for the east-west bound links in the first pattern of the OD matrix; 1 for otherwise
w_{cp}	10

The RL policy network comprises two fully connected layers, each with 32 neurons.

RL models undergo training across multiple episodes, each simulating 16,200 seconds—including an 1,800-second warm-up phase. During warm-up, the signal scheme remains unchanged, and vehicles are gradually introduced into the road network to ensure a stable initial state. Each episode contains 144 steps, derived by dividing the post-warm-up duration (16,200 - 1,800 seconds) by the control interval.

The RLlib library is employed for learning the signal control policy.

This research employs a high-performance computing platform equipped with an Intel Core i9-14900K processor, featuring 8 high-performance cores and 16 energy-efficient cores, enabling 32 threads in total. Additionally, the platform is integrated with an NVIDIA RTX A6000 48GB graphics card.

5.SIMULATION RESULTS AND DISCUSSIONS

5.1 Hyperparameter tuning for DreamerV3

For DreamerV3, two hyperparameters demand tuning: the training ratio (ratio of replayed steps to environment steps) and model size. Higher training ratios generally boost data efficiency. As per literature (12), focusing on model size S suffices, and prioritizing a medium - scale training ratio cuts hyperparameter - tuning time notably.

Figure 8(a) presents training curves of S - sized models with training ratios 64, 128, 256 when the reward solely targets congestion relief. To clarify end - training performance, curves post - 36 hours are magnified. All ratios finish training within 48 hours; as per DreamerV3 literature (13), larger ratios let the model reach higher episode rewards faster.

Figure 8(b) shows curves for the same S - sized models and ratios under a reward function that combines congestion relief and total travel time minimization. A similar pattern holds: all ratios complete training within 48 hours despite the more complex reward, and larger ratios usually speed up getting higher rewards. A slight difference is that the ratio - 64 curve has significant fluctuations, with occasional large swings lingering near the training end.

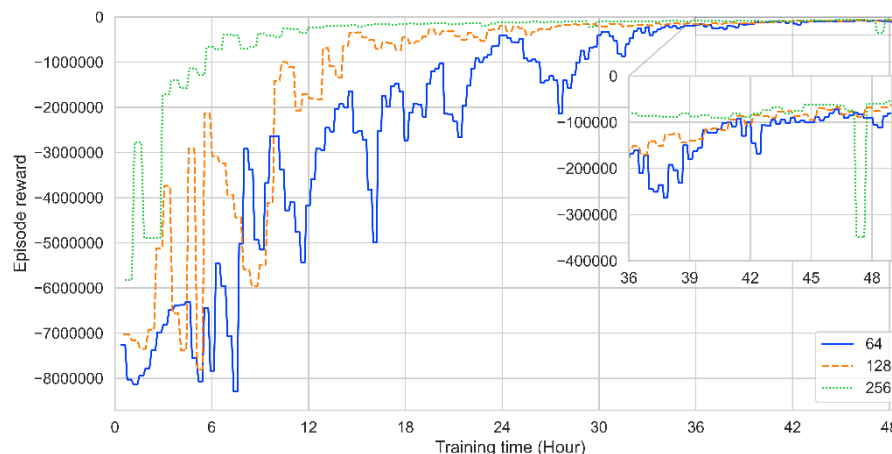


Figure 8 (a) Learning process (Scenario 1)

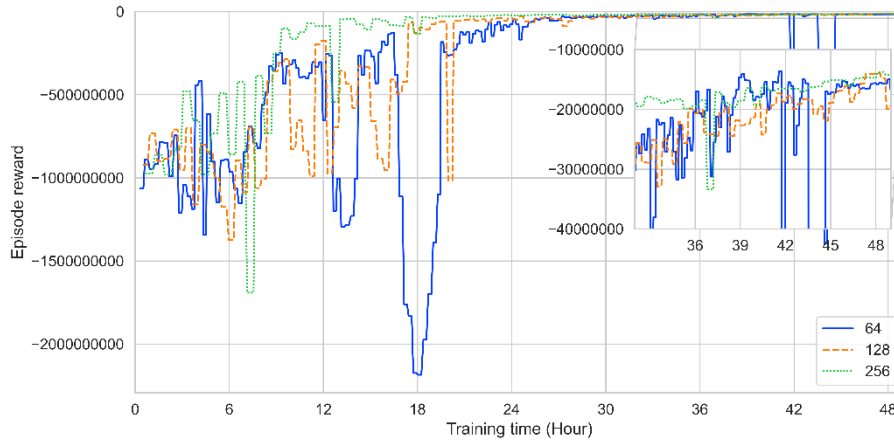


Figure 8(b). Learning process (Scenario 2)

5.2 Performance of TSC

The Traffic Signal Control (TSC) model's performance under demand-fluctuation scenarios was evaluated against a baseline with unadjusted signal timings. Multi-dimensional OD demand fluctuations were generated from the original fixed OD matrix via random sampling and parameter adjustment: for each OD pair, a random number (1-100) determined the fluctuation direction. If >50 , traffic volume increased: per 10%, 20%, 30% ratios, k vehicles ($k = \text{original count} \times \text{ratio}$) were randomly sampled, duplicated with modified IDs (e.g., append "A"), and their departure times adjusted ($\pm 1s$) to avoid full temporal overlap, simulating real traffic's time dispersion. If <50 , volume decreased: m vehicles ($m = \text{original count} \times (1 - \text{ratio})$) were retained, excess removed randomly, preserving the original time distribution to maintain initial traffic temporal features.

Three fluctuation scenarios (Table 3) were injected in real-time during inference (post 1,800s simulation/warm-up). Training used only the fixed OD matrix to ensure no prior knowledge of fluctuations, relying on the model's decision mechanism. Each fluctuation level was tested 5 times to reduce randomness; data were aggregated into comparative bar charts.

Figure 10 presents the distribution characteristics of queue lengths under the original fixed OD matrix (defined as the baseline scenario). The results indicate that queue lengths are dominantly clustered in the low - value range (e.g.

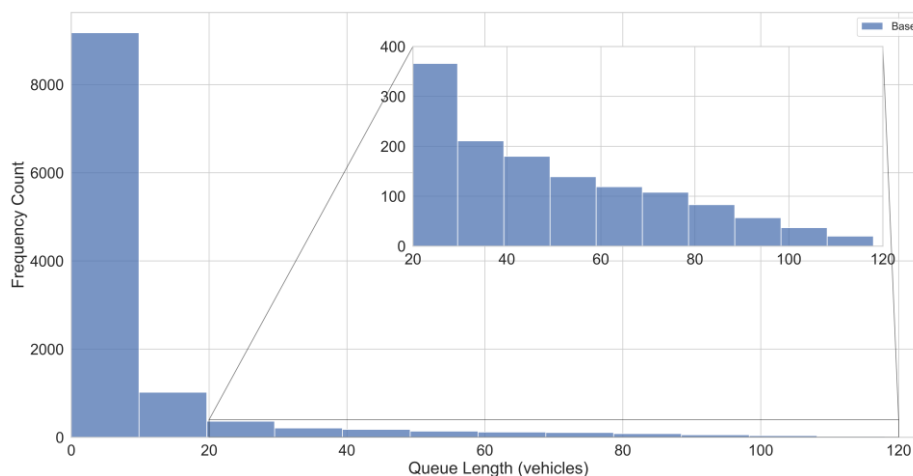
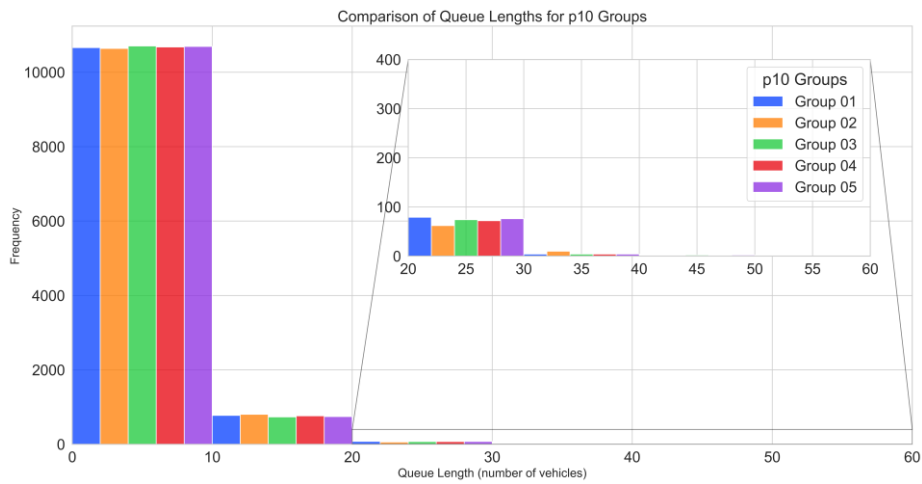


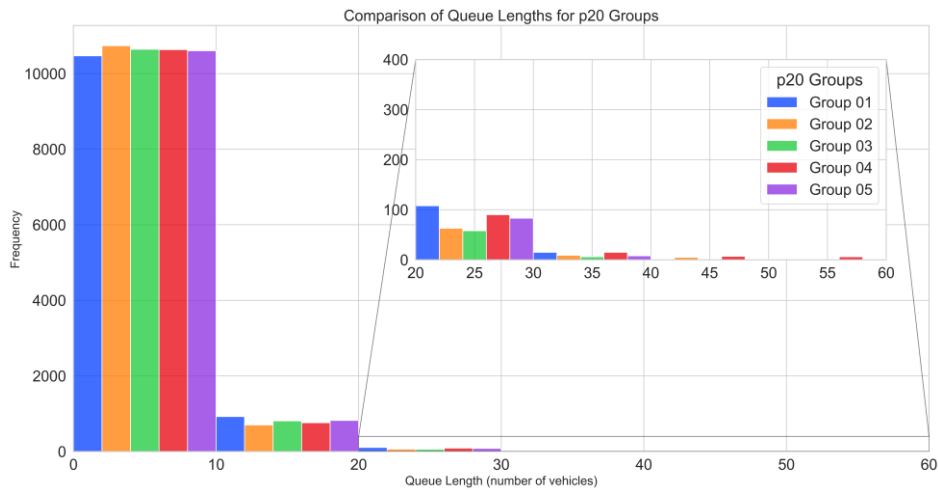
Figure 10. Queue length frequency distribution under baseline (unoptimized) conditions.

For the three subsequent figures (corresponding to 10%, 20%, and 30% demand fluctuation scenarios), demand fluctuations significantly alter the queue length distribution characteristics. Under the 10% demand fluctuation (p10 Groups), the frequency of queue lengths in the mid - range (e.g., 20 - 40 vehicles) increases compared to the baseline, indicating that even a small - scale demand change can disrupt traffic flow stability.

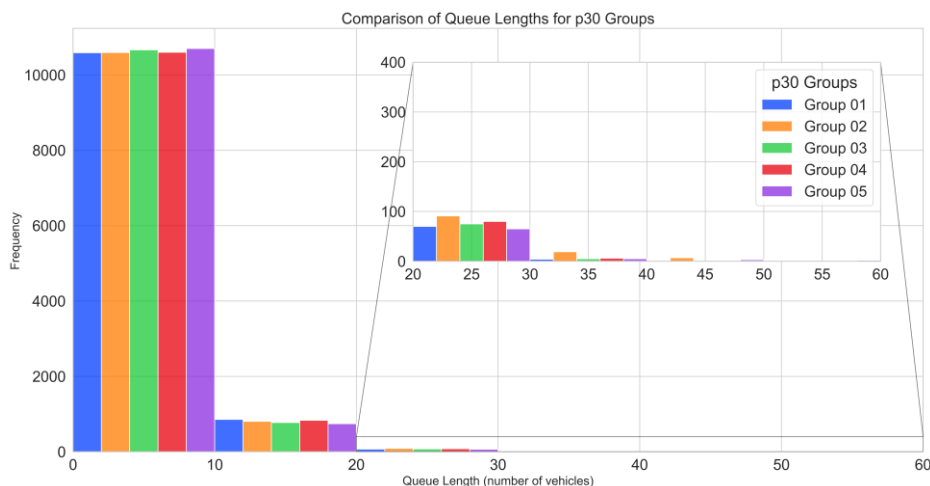
As the fluctuation amplitude rises to 20% (p20 Groups) and 30% (p30 Groups), the queue length distribution shifts further towards higher values. The frequency of moderate to heavy congestion (queue length ≥ 25 vehicles) increases continuously, and the distribution becomes more dispersed. This reflects that larger demand fluctuations impose greater pressure on the traffic system, leading to more frequent and severe queuing phenomena.



(a) 10% (p₁₀)



(b) 20% (p₂₀)



(c)30% (p_30)

Figure11. Queue length frequency distributions across control groups under varying OD demand fluctuations

In summary, the TSC model (implicit in the demand - fluctuation generation and result observation) faces challenges in maintaining stable traffic flow under demand fluctuations. The queue length distribution characteristics under different fluctuation amplitudes can help in further optimizing the model's decision - making mechanism to adapt to dynamic traffic demand changes, thereby enhancing the efficiency of urban traffic signal control.

6.CONCLUSIONThis

This study innovatively develops a single-agent reinforcement learning (RL) framework for regional traffic signal control (TSC). Adopting a centralized decision-making paradigm, it avoids the inherent coordination complexities of multi-agent systems. The model uses an adjacency matrix to uniformly encode road network topology, real-time queue states from probe vehicles, and signal timing parameters. Leveraging the efficient learning ability of the DreamerV3 world model, the framework maintains stable performance even in inference scenarios with 30% origin-destination (OD) demand fluctuations. Experiments show that this architecture has significant advantages in reducing queue lengths and enhancing disturbance resistance, establishing a new paradigm for intelligent traffic control driven by probe vehicle technology.

Future research will focus on two directions to improve practical applicability: First, introducing stochastic OD demand fluctuations during the training phase to build a dynamic environment simulating real-world traffic uncertainty, and systematically evaluating the model's convergence and ability to achieve control objectives in continuously changing scenarios. Second, exploring regional collaborative optimization mechanisms under contingency events (e.g., accidents, extreme weather), and enhancing the system's emergency response capabilities through signal priority strategies and dynamic allocation of network resources. These improvements will promote the practical deployment of the theoretical model in complex urban environments, providing more robust decision support for intelligent traffic management.

DATA AVAILABILITY

The data that support the findings of this study are available from the author, Qiang Li (liqiangjl@qq.com), upon reasonable request.

CONFLICTS OF Interest

The authors declare that there are no conflicts of interest related to the publication of this paper.

ACKNOWLEDGMENTS

This study was supported by a grant from Guangdong Province General Regular Projects of Social Sciences Planning (No. GD24CGL37), Natural Science Foundation of Top Talent of SZTU (No. GDRC202322).

REFERENCES

1. H. Wei, G. Zheng, V. Gayah, and Z. Li, “A Survey on Traffic Signal Control Methods,” 2020, [Online]. Available: <http://arxiv.org/abs/1904.08117>
2. C. Wu, I. Kim, and Z. Ma, “Deep Reinforcement Learning Based Traffic Signal Control: A Comparative Analysis,” *Procedia Computer Science*, vol. 220, pp. 275–282, 2023, <https://doi.org/10.1016/j.procs.2023.03.036>.
3. K. Arulkumaran, M. P. Deisenroth, M. Brundage, and A. A. Bharath, “Deep Reinforcement Learning: A Brief Survey,” *IEEE Signal Processing Magazine*, vol. 34, no. 6, pp. 26–38, 2017, <https://doi.org/10.1109/MSP.2017.2743240>.
4. D. Li, J. Wu, M. Xu, Z. Wang, and K. Hu, “Adaptive Traffic Signal Control Model on Intersections Based on Deep Reinforcement Learning,” *Journal of Advanced Transportation*, vol. 2020, Aug. 2020, <https://doi.org/10.1155/2020/6505893>.
5. L. Zheng and B. Wu, “A Reinforcement Learning Based Traffic Control Strategy in a Macroscopic Fundamental Diagram Region,” *Journal of Advanced Transportation*, vol. 2022, Apr. 2022, <https://doi.org/10.1155/2022/5681234>.
6. A. Haydari and Y. Yilmaz, “Deep Reinforcement Learning for Intelligent Transportation Systems: A Survey,” *IEEE Transactions on Intelligent Transportation Systems*, vol. 23, no. 1, pp. 11–32, 2022, <https://doi.org/10.1109/TITS.2020.3008612>.
7. M. Noaen *et al.*, “Reinforcement learning in urban network traffic signal control: A systematic literature review,” *Expert Systems with Applications*, vol. 199, p. 116830, Aug. 2022, <https://doi.org/10.1016/j.eswa.2022.116830>.
8. H. Wei and G. Zheng, “Recent Advances in Reinforcement Learning for Traffic Signal Control,” *ACM SIGKDD Explorations Newsletter*, vol. 22, pp. 12–18, 2021, [Online]. Available: <https://api.semanticscholar.org/CorpusID:229540095>.
9. H. Zhao, C. Dong, J. Cao, and Q. Chen, “A survey on deep reinforcement learning approaches for traffic signal control,” *Engineering Applications of Artificial*

- Intelligence*, vol. 133, p. 108100, Jul. 2024, <https://doi.org/10.1016/j.engappai.2024.108100>.
10. C. Chen *et al.*, “Toward A Thousand Lights: Decentralized Deep Reinforcement Learning for Large-Scale Traffic Signal Control,” in *Proceedings of the AAAI Conference on Artificial Intelligence*, Apr. 2020, pp. 3414–3421. <https://doi.org/10.1609/aaai.v34i04.5744>.
 11. F. Lian, B. Chen, K. Zhang, L. Miao, J. Wu, and S. Luan, “Adaptive traffic signal control algorithms based on probe vehicle data,” *Journal of Intelligent Transportation Systems*, vol. 25, no. 1, pp. 41–57, Jan. 2021, <https://doi.org/10.1080/15472450.2020.1750384>.
 12. Q. Li, H. Hu, and L. Miao, “Queue Length Estimation Using Probe Vehicle Data for a Congested Arterial Road,” in *CICTP 2015 - Efficient, Safe, and Green Multimodal Transportation - Proceedings of the 15th COTA International Conference of Transportation Professionals*, Beijing, China, 2015, pp. 2295–2306. [Online]. Available: <http://dx.doi.org/10.1061/9780784479292.213>.
 13. J. J. Henry, J. L. Farges, and J. Tuffal, “The Prodyn Real Time Traffic Algorithm,” *IFAC Proceedings Volumes*, vol. 16, no. 4, pp. 305–310, Apr. 1983, [https://doi.org/10.1016/S1474-6670\(17\)62577-1](https://doi.org/10.1016/S1474-6670(17)62577-1).
 14. H. Ceylan and M. G. H. Bell, “Traffic signal timing optimisation based on genetic algorithm approach, including drivers’ routing,” *Transportation Research Part B: Methodological*, vol. 38, no. 4, pp. 329–342, 2004, doi: [https://doi.org/10.1016/S0191-2615\(03\)00015-8](https://doi.org/10.1016/S0191-2615(03)00015-8).
 15. K. Pandit, D. Ghosal, H. M. Zhang, and C.-N. Chuah, “Adaptive Traffic Signal Control With Vehicular Ad hoc Networks,” *IEEE Transactions on Vehicular Technology*, vol. 62, no. 4, pp. 1459–1471, 2013, <https://doi.org/10.1109/TVT.2013.2241460>.
 16. J. Little, M. Kelson, and N. Gartner, “MAXBAND: A Program for Setting Signals on Arteries and Triangular Networks,” *Transportation Research Record Journal of the Transportation Research Board*, vol. 795, pp. 40–46, Dec. 1981, <https://dspace.mit.edu/handle/1721.1/1979>.
 17. K. Zhang, Z. Cui, and W. Ma, “A survey on reinforcement learning-based control for signalized intersections with connected automated vehicles,” *Transport Reviews*, vol. 44, no. 6, pp. 1187–1208, Nov. 2024, <https://doi.org/10.1080/01441647.2024.2377637>.
 18. T. Chu, J. Wang, L. Codeca, and Z. Li, “Multi-Agent Deep Reinforcement Learning for Large-Scale Traffic Signal Control,” *IEEE Transactions on Intelligent Transportation Systems*, vol. 21, no. 3, pp. 1086–1095, Mar. 2020, <https://doi.org/10.1109/TITS.2019.2901791>.
 19. H. Wei *et al.*, “PressLight: Learning Max Pressure Control to Coordinate Traffic Signals in Arterial Network,” in *Proceedings of the 25th ACM SIGKDD International Conference on Knowledge Discovery & Data Mining*, Anchorage AK USA: ACM, Jul. 2019, pp. 1290–1298.

- <https://doi.org/10.1145/3292500.3330949>.
20. P. Varaiya, “Max pressure control of a network of signalized intersections,” *Transportation Research Part C: Emerging Technologies*, vol. 36, pp. 177–195, Nov. 2013, <https://doi.org/10.1016/j.trc.2013.08.014>.
 21. R. Bokade, X. Jin, and C. Amato, “Multi-Agent Reinforcement Learning Based on Representational Communication for Large-Scale Traffic Signal Control,” *IEEE Access*, vol. 11, pp. 47646–47658, 2023, <https://doi.org/10.1109/ACCESS.2023.3275883>.
 22. L. Yan *et al.*, “Graph cooperation deep reinforcement learning for ecological urban traffic signal control,” *Applied Intelligence*, vol. 53, no. 6, pp. 6248–6265, Mar. 2023, <https://doi.org/10.1007/s10489-022-03208-w>.
 23. J. Ma and F. Wu, “Learning to Coordinate Traffic Signals With Adaptive Network Partition,” *IEEE Transactions on Intelligent Transportation Systems*, vol. 25, no. 1, pp. 263–274, Jan. 2024, <https://doi.org/10.1109/TITS.2023.3308594>.
 24. Noaen, Mohammad , et al."Reinforcement learning in urban network traffic signal control: A systematic literature review".EXPERT SYSTEMS WITH APPLICATIONS,199(0): ,<https://doi.org/10.1016/j.eswa.2022.116830>
 25. Zhang, Kaiwen , et al."A survey on reinforcement learning-based control for signalized intersections with connected automated vehicles".TRANSPORT REVIEWS,44(6):1187-1208,<https://doi.org/10.1080/01441647.2024.2377637>
 26. Q. Li, T. Miwa, and T. Morikawa, “Efficient link travel time estimation for signalized link by small size probe reports,” in *Proceedings of the 9th International Conference of Chinese Transportation Professionals, ICCTP 2009: Critical Issues in Transportation System Planning, Development, and Management*, Harbin, China, 2009, pp. 1884–1891. [Online]. Available: [http://dx.doi.org/10.1061/41064\(358\)265](http://dx.doi.org/10.1061/41064(358)265).
 27. M. Towers *et al.*, “Gymnasium: A Standard Interface for Reinforcement Learning Environments,” *arXiv preprint arXiv:2407.17032*, 2024. [Online]. Available: <https://arxiv.org/abs/2407.17032>.
 28. Hafner, D., J. Pasukonis, J. Ba, and T. Lillicrap, “Mastering Diverse Domains through World Models,” *arXiv preprint arXiv:2301.04104*, 2023. <https://doi.org/10.48550/arXiv.2301.04104>.
 29. Hafner, D., T. Lillicrap, M. Norouzi, and J. Ba, “Mastering Atari with Discrete World Models,” *arXiv preprint arXiv:2010.02193*, 2020. <https://doi.org/10.48550/arXiv.2010.02193>.
 30. Hafner, D., T. Lillicrap, J. Ba, and M. Norouzi, “Dream to Control: Learning Behaviors by Latent Imagination,” *arXiv preprint arXiv:1912.01603*, 2019. <https://doi.org/10.48550/arXiv.1912.01603>.
 31. Ha, D., and J. Schmidhuber, “World Models,” *arXiv preprint arXiv:1803.10122*, 2018. <https://doi.org/10.48550/arXiv.1803.10122>.